

			Form Approved OMB NO. 0704-0188	
Public Reporting burden for this collection of information is estimated to average 1 hour per response, including the time for reviewing instructions, searching existing data sources, gathering and maintaining the data needed, and completing and reviewing the collection of information. Send comment regarding this burden estimates or any other aspect of this collection of information, including suggestions for reducing this burden, to Washington Headquarters Services, Directorate for Information Operations and Reports, 1215 Jefferson Davis Highway, Suite 1204, Arlington, VA 22202-4302, and to the Office of Management and Budget, Paperwork Reduction Project (0704-0188,) Washington, DC 20503.				
1. AGENCY USE ONLY (Leave Blank)		2. REPORT DATE		3. REPORT TYPE AND DATES COVERED Final 22Jul02 - 30June 06
4. TITLE AND SUBTITLE Development of Design Criteria for Highly Efficient Fuel Cells			5. FUNDING NUMBERS DAAD19-02-1-0311	
6. AUTHOR(S) Stimming, Ulrich				
7. PERFORMING ORGANIZATION NAME(S) AND ADDRESS(ES) Technical University of Munich			8. PERFORMING ORGANIZATION REPORT NUMBER	
9. SPONSORING / MONITORING AGENCY NAME(S) AND ADDRESS(ES) U. S. Army Research Office P.O. Box 12211 Research Triangle Park, NC 27709-2211			10. SPONSORING / MONITORING AGENCY REPORT NUMBER 44279.2-CH	
11. SUPPLEMENTARY NOTES The views, opinions and/or findings contained in this report are those of the author(s) and should not be construed as an official Department of the Army position, policy or decision, unless so designated by other documentation.				
12 a. DISTRIBUTION / AVAILABILITY STATEMENT Approved for public release; distribution unlimited.			12 b. DISTRIBUTION CODE	
13. ABSTRACT (Maximum 200 words) See Attached Report				
14. SUBJECT TERMS			15. NUMBER OF PAGES	
			16. PRICE CODE	
17. SECURITY CLASSIFICATION OR REPORT UNCLASSIFIED	18. SECURITY CLASSIFICATION ON THIS PAGE UNCLASSIFIED	19. SECURITY CLASSIFICATION OF ABSTRACT UNCLASSIFIED	20. LIMITATION OF ABSTRACT UL	

NSN 7540-01-280-5500

Standard Form 298 (Rev.2-89)
Prescribed by ANSI Std. Z39-18
298-102

Enclosure 1

Final Progress Report (Jan. 2002 to Aug. 2005)

Introduction

Catalytic activity of islands and single clusters prepared on different substrates using either delocalized deposition pulse technique or tip induced deposition in a electrochemical scanning tunneling microscope (EC – STM) was studied in order to determine the optimal size and distribution of catalytic active metals. Activity at these islands, single clusters, as well as cluster arrays has been measured in situ immediately after preparation to avoid degeneration. In case of single Pd clusters and cluster arrays, our new developed technique utilizing an STM tip for local reactivity measurements has been applied. Furthermore, a novel preparation procedure for catalytically active nanoprobles has been developed to apply the pH – sensing effect of hydrogen loaded Pd in future investigations.

Pd on Au(111):

The influence of the substrate on the properties of Pd ad layers on Au(111) was investigated as a function of the morphology of the Pd deposits (Fig. 1). The relation between the binding energy of d-electrons of Pd on Au(111) and their activity regarding proton reduction in aqueous perchloric solution was investigated by X-ray photoelectron spectroscopy and galvanostatic reactivity measurements. Morphology and stability of epitaxially grown Pd layers and sub-monolayers on Au(111) were characterized by cyclic voltammetry and scanning tunneling microscopy prior and after the reactivity measurements. The proton reduction rate increases with decreasing thickness of the Pd layers from 3 to 1 ML by a factor of three, much smaller than predicted by Nørskov. By contrast, at Pd coverage below 1 ML the proton reduction rate increases by up to one order of magnitude, which may

confirm an additional contribution of the spill over of hydrogen onto the Au(111) terraces (Fig. 2).

Pd coverage below 1 monolayer (ML) show an increase of the proton reduction rate by up to one order of magnitude, compared to a single ML of Pd on Au(111). In order to proof this, Pd ad layers on Au(111) were prepared with a small island size distribution and different island density using a two step potential pulse technique. During a first nucleation step clusters were formed on Au(111). The applied over potential of this first step determines the density of particles. In a subsequent growth step these nuclei were grown to larger particles with the desired size. Thus, an independent variation of size and density of Pd islands on Au(111) can be derived varying over potential within the first and time in the second step. So far, the distribution of island diameters, as determined from in-situ scanning tunneling microscopy (STM) measurements, could be improved to have size values of approximately 1 – 1.5 nm, and maxima below 2 nm. The morphology and stability of these Pd islands on Au(111) were characterized by cyclic voltammetry and STM prior and after the reactivity measurements. The activity of samples showing very small cluster diameters and very small size distribution at low coverage is increased by up to one order of magnitude as compared to our previous findings at samples showing larger Pd islands. Thus, the activity data for Pd islands seem to increase further with decreasing cluster size, and, thus, converge with the activity data derived from our activity measurements at single clusters utilizing our previously developed in-situ technique for local activity measurements (Fig. 3). This technique measures hydrogen oxidation current at the STM tip, which results from the hydrogen produced by proton reduction at the Pd cluster or cluster array on Au(111) underneath the STM tip (Fig. 4).

In order to separate effects of electronic modification of terrace atoms in the nano islands from effects of edge atoms the dependence of proton reduction rate as a function of

the ratio of edge atoms vs. terrace atoms of the Pd islands has been investigated by varying the size of the islands. The influence of the edge atoms of the Pd islands on the proton reduction rate at Pd islands on Au(111) has been found to be small and not significant.

Single clusters and cluster arrays consisting of clusters with same size have been fabricated utilizing the well known tip induced deposition procedure (Fig.5). A Pd loaded Au or Pt tip (Fig. 6) is approached towards the substrate until it gently touches the surface and a “jump to contact” occurs resulting in a localized cluster deposition underneath the tip (Fig 7). After deposition of a defined number of clusters their activity was determined using our previously developed in-situ technique for local activity measurements (Fig. 3). It is found for arrays consisting of a few Pd clusters, that the current measured for Pd cluster arrays at a particular overpotential increases not linearly with the number of clusters in the array (Fig. 8). Moreover, we found a dependence of the deposited clusters on the cluster separation. The distance between the clusters seems to have an optimum for catalytic activity. Since the increased activity of single Pd clusters should be caused by the shift in the center of the d-band and the spill over effect of hydrogen evolved at the Pd cluster, which diffuses onto the surrounding Au(111) terraces where it finally desorbs into the electrolyte, variations in the hydrogen evolution current are expected due to the separation of the Pd clusters on the same Au(111) surface.

Pd on Cu surfaces:

Pd clusters have been prepared on different single crystal Cu surfaces utilizing the above mentioned deposition routine (Fig. 9 and Fig. 10). The d-band model by Hammer and Nørskov predicts a change in activity due to the magnitude and the sign of mismatch in the lattice constants. The lattice constant of Cu is somewhat smaller than that of Pd leading to a

slight compression in the Pd layer in contrast to Pd on Au where the Pd –Pd distance is increased by approx. 5%. Consequently, we find in contrast to the high activity of Pd clusters on Au(111), that Pd clusters on Cu(111), Cu(110), and Cu(100) surfaces show an activity that is not enhanced as found for Pd on Au. This result is expected from the d-band model by Nørskov [1,2].

Development of a pH sensitive nanosensor:

In addition to the indirect technique of measuring local reactivity of a Pd cluster using the reverse catalytic reaction current at the STM tip, a second technique to locally characterize catalytic activity has been developed, using STM tips as local pH sensors. A direct technique allows characterizing reactions, where a product cannot be detected by a reverse reaction. We will use this technique for investigations of methanol oxidation, oxygen reduction, and proton reduction (in comparison to the indirect technique). The STM tip sensors are prepared from Pd wire by electrochemical etching and subsequent saturation with H₂ (Fig. 11). They show an open cell potential which is determined by the proton concentration at the STM tip position. In order to calibrate the pH sensing hydrogen loaded Pd tip, we developed a calibration graph utilizing a commercially available pH sensor (Fig. 11). The obtained calibration curves allow use to apply this technique in the EC – STM. The local volume which can be probed by this technique is as small as approximately 10⁻¹⁵ cm³. The stability of hydrogen loaded Pd tips has been proven to be suitable for precision in-situ measurements of local proton concentration around an active metal cluster. STM tip isolation results presently in a small degradation of sensor performance, which still must be optimized. First in-situ measurements of local changes in proton concentration above active Pd clusters on Au(111) were performed using an newly developed amplifier in the STM circuitry. An important

advantage of this type of proton concentration sensor is the fact that it can be also used as STM tip for imaging of the surface morphology in a single experiment.

List of Appendix, Illustrations and Tables

Illustrations:

- Fig. 1: EC - STM images of different Pd loadings on Au(111) in order to investigate the influence of island density, edge atoms and island diameter.
- Fig. 2: Obtained hydrogen evolution current densities: comparison between different Pd loadings on Au(111).
- Fig. 3: Principles of the novel developed measuring technique.
- Fig. 4: Distance relationship investigations in order to determine diffusion constants of the involved reactants (upper graph). Current transients due to the hydrogen evolution of the deposited clusters measured at the unisolated tip apex (lower graph).
- Fig. 5: Schematic of the cluster deposition routine.
- Fig. 6: Cyclic voltammogram of Pd deposition and dissolution on a gold tip (left) and Scanning-Electron-Microscope image (right) of deposited Pd on a electrochemically etched and isolated Au tip.
- Fig. 7: Subsequent deposition of three Pd clusters on Au(111).
- Fig. 8: Different current densities of three subsequently deposited Pd clusters on Au(111). The hydrogen evolution investigations utilizing the novel developed measurement technique reveals a different hydrogen evolution behaviour for varying number of clusters.
- Fig. 9: Subsequent deposition of several Pt clusters on Cu (upper images). Stability investigations of three Pt clusters on Cu (lower images).

- Fig. 10: Example images showing the different stages of optimization of the Pd - nanoprobe preparation technique. The Pd tip etched with 1,45 V seems to have the best shape to combine local ph – sensing techniques with the electrochemical STM. Furthermore, the Pd tip can additionally be used as generator electrode to deposit localized nanostructures.
- Fig. 11: The comparison of different ph - values measured with an commercially available ph – sensor and the obtained open cell potential of a hydrogen loaded pd wire led to a calibration graph for ph – sensing (left). The normalized and fitted graph to the right shows the dependence of the open cell potential on the ph – value for a hydrogen loaded Pd wire.

Publications:

- J. Meier, K.A. Friedrich, U. Stimming, *Faraday Discuss.*, **121** (2002) 365.
- M. Del Popolo, E. Leiva, H. Kleine, J. Meier, U. Stimming, M. Mariscal, and W. Schmickler, *Appl. Phys. Lett.*, **81** (2002) 2635.
- M. Eikerling, J. Meier, U. Stimming, *Z. Phys. Chem.* **217** (2003) 395.
- M. Del Popolo, E. Leiva, H. Kleine, J. Meier, U. Stimming, M. Mariscal, and W. Schmickler, *Electrochim. Acta*, **81** (2003) 1287.
- J. Meier, J. Schiotz, P. Liu, J. K. Nørskov, U. Stimming, *Chem. Phys. Lett.*, **390** (2004) 440.
- J. K. Nørskov, T. Bligaard, A. Logadottir, J. R. Kitchin, J. G. Chen, S. Pandelov and U. Stimming, *J. Electrochem Soc.* **152** (2005) J23-J26.
- S. Pandelov, and U. Stimming, submitted for publication.
- S. Pandelov, and U. Stimming, *in preparation*.

Technical reports submitted to ARO

Interim Technical Report: July 2002 – January 2003

Interim Technical Report: January 2003 – January 2004

Interim Technical Report: January 2004 – January 2005

Interim Technical Report: January 2005 – August 2005

List of all participating scientific personnel (earned degrees)

Dr. Jürgen Meier, Ph.D. (2003).

Christian Camus, *diploma thesis* (2004)

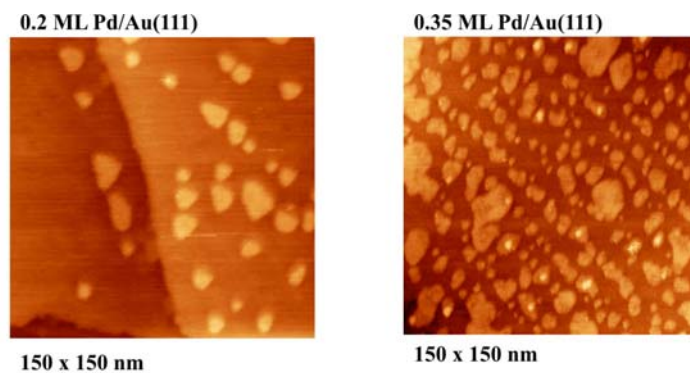
Stanislav Pandelov, Ph.D. anticipated 2006

Bibliography

[1] B. Hammer and J.K. Nørskov, *Surf.Sci.* **343** (1995) 211

[2] C. Camus, *diploma thesis* (2004).

Appendixes



ML Pd/Au(111)	average island diameter [nm]	island density [island/cm ²] $\times 10^{11}$	edge atoms/surface atoms [%]
0.2	10.2	1	1.65
0.35	7.8	8.9	3.47

Fig. 1: EC - STM images of different Pd loadings on Au(111) in order to investigate the influence of island density, edge atoms and island diameter.

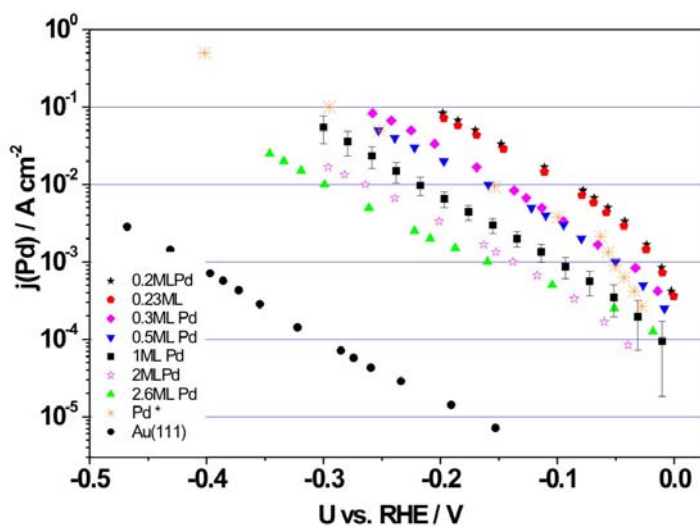


Fig. 2: Obtained hydrogen evolution current densities: Comparison between different Pd coverage on Au(111).

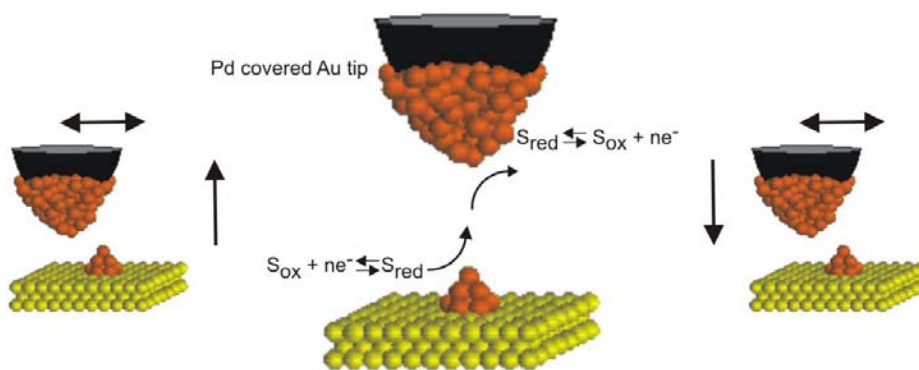


Fig. 3: Principles of the novel developed measuring technique.

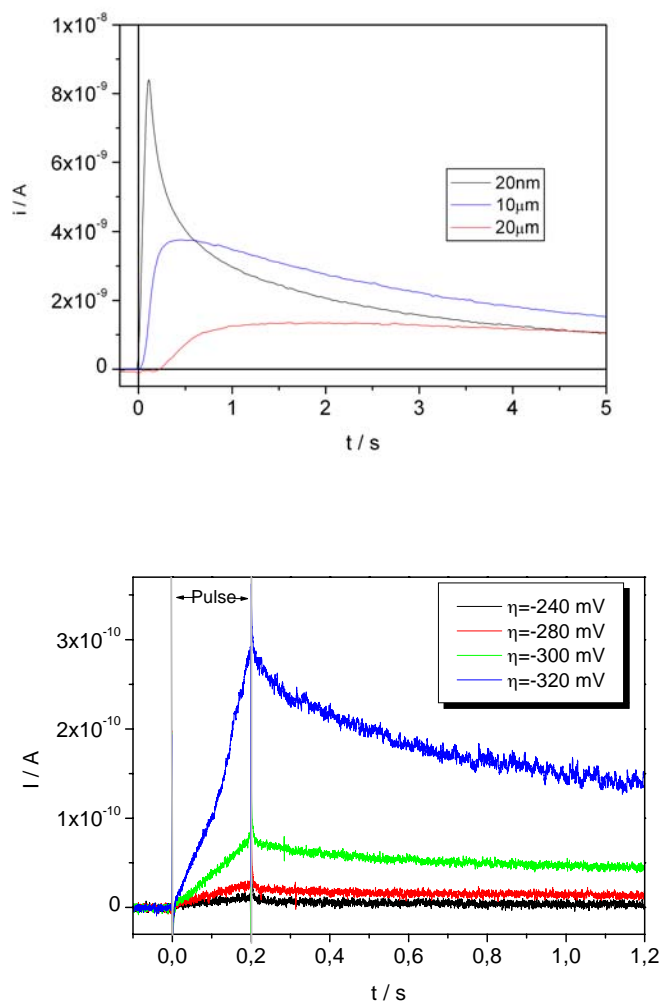


Fig. 4: Distance relationship investigations in order to determine diffusion constants of the involved reactants (upper graph). Current transients due to the hydrogen evolution of the deposited clusters measured at the unisolated tip apex (lower graph).

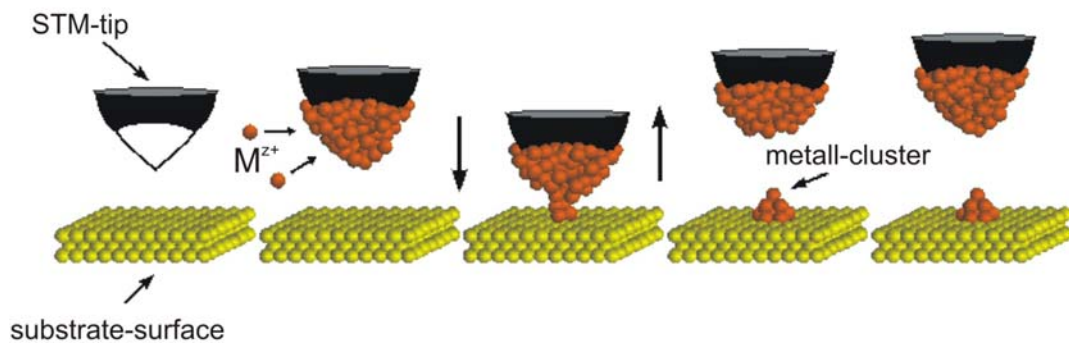


Fig. 5: Schematic of the cluster deposition routine.

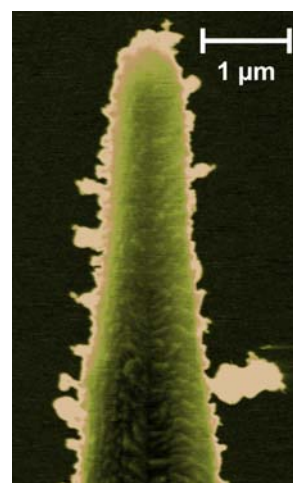
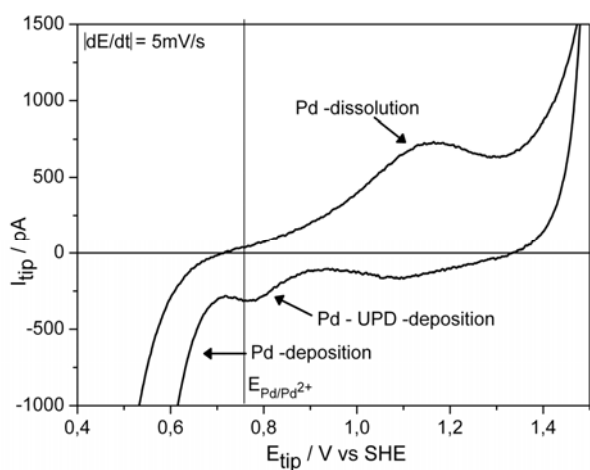


Fig. 6: Cyclic voltammogram of Pd deposition and dissolution on a gold tip (left) and Scanning-Electron-Microscope image (right) of deposited Pd on a electrochemically etched and isolated Au tip.

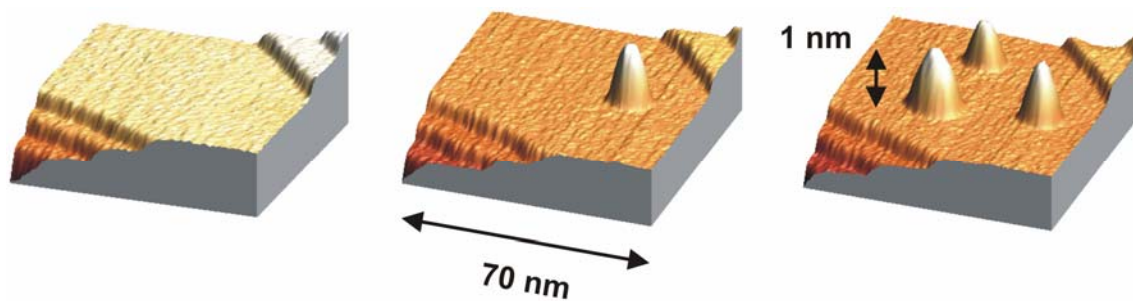


Fig. 7: Subsequent deposition of three Pd clusters on Au(111).

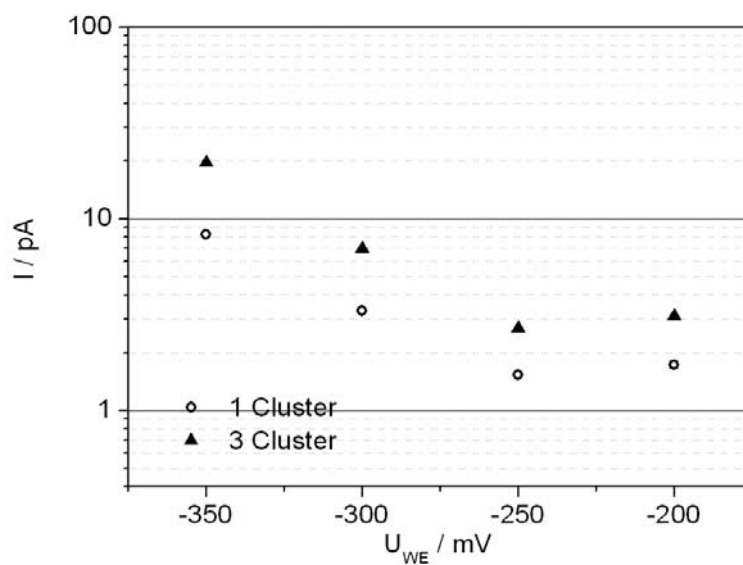


Fig. 8: Different current densities of three subsequently deposited Pd clusters on Au(111). The hydrogen evolution investigations utilizing the novel developed measurement technique reveals different hydrogen evolution rates for varying number of clusters.

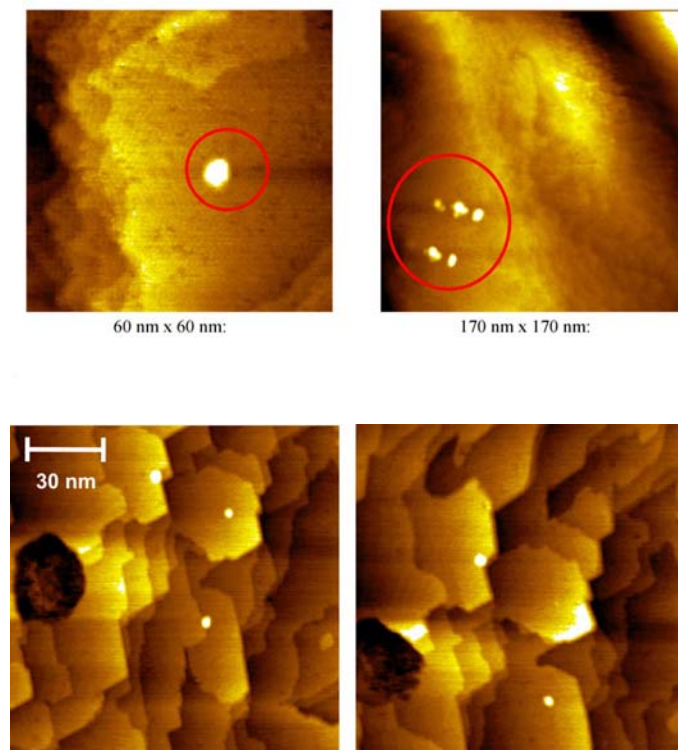


Fig. 9: Subsequent deposition of several Pt clusters on Cu (upper images). Stability investigations of three Pt clusters on Cu (lower images).

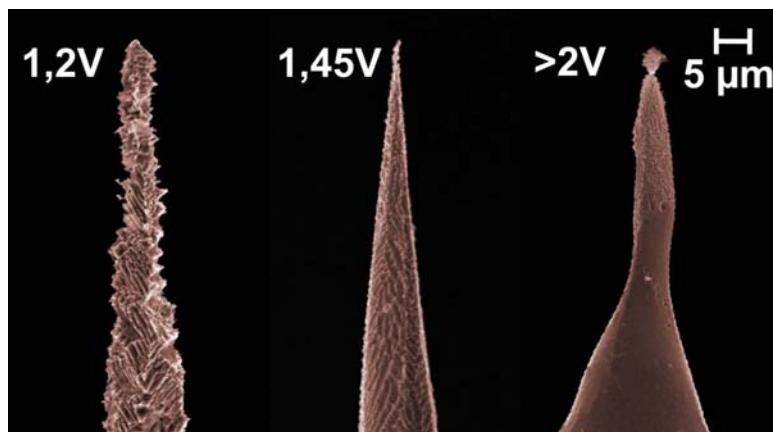


Fig. 10: Example images showing the different stages of optimization of the Pd - nanoprobe preparation technique. The Pd tip etched with 1.45 V seems to have the best shape to combine local pH sensing techniques with the electrochemical STM. Furthermore, the Pd tip can additionally be used as generator electrode to deposit localized nanostructures.

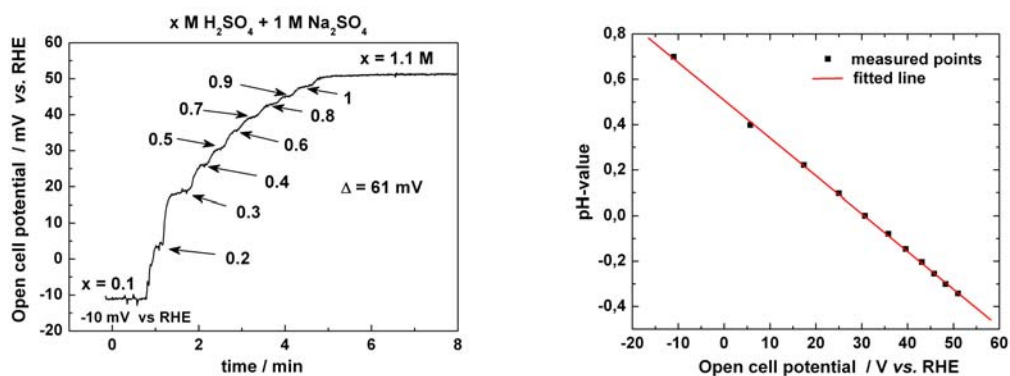


Fig. 11: The comparison of different pH values measured with a commercially available pH sensor and the obtained open cell potential of a hydrogen loaded Pd wire led to a calibration graph for pH sensing (left). The normalized and fitted graph to the right shows the dependence of the open cell potential on the pH value for a hydrogen loaded Pd wire.